

Astrophysical $S_{17}(0)$ factor extraction from breakup of ${}^8\text{B}$ on ${}^{58}\text{Ni}$ at energies near the Coulomb barrier

T. L. Belyaeva,¹ E. F. Aguilera,² E. Martinez-Quiroz,² A. M. Moro,³ and J. J. Kolata⁴

¹Universidad Autónoma del Estado de México, Código Postal 50000, Toluca, México

²Departamento del Acelerador, Instituto Nacional de Investigaciones Nucleares, A.P. 18-1027, Código Postal 11801 Mexico, Mexico

³Departamento de Física Atómica, Molecular y Nuclear, Universidad de Sevilla, Post Office Box 1065, E-41080 Sevilla, Spain

⁴Physics Department, University of Notre Dame, Notre Dame, Indiana 46556, USA

(Received 8 October 2009; published 31 December 2009)

We have performed continuum-discretized coupled channels (CDCC) calculations of the breakup of ${}^8\text{B}$ on ${}^{58}\text{Ni}$ and direct proton transfer for the ${}^8\text{B} + {}^{58}\text{Ni}$ system at laboratory energies of 20–28.4 MeV. The influence of the ${}^7\text{Be}$ core-target optical potential (OP) on the breakup cross section was investigated. Elastic scattering angular distributions for the ${}^7\text{Be} + {}^{58}\text{Ni}$ and ${}^8\text{B} + {}^{58}\text{Ni}$ systems at five different energies around the Coulomb barrier were studied, and a reasonable energy-independent OP for each system was obtained. Using these OPs and two different ${}^7\text{Be}$ - p relative motion wave functions, and summing breakup and direct proton transfer contributions, we were able to fit the experimental cross section at a ${}^8\text{B}$ laboratory energy of 25.75 MeV. We calculated the excitation function for the ${}^7\text{Be}$ emission in the ${}^8\text{B} + {}^{58}\text{Ni}$ reaction, where ${}^7\text{Be}$ products were measured at the forward angle $\theta_{\text{lab}} = 45^\circ$ in the energy interval $E_{\text{lab}} = 20\text{--}28.4$ MeV. In view of the peripheral character of the ${}^8\text{B}$ breakup reaction at near-barrier energies, we could extract the asymptotic normalization coefficient for the ${}^7\text{Be}$ - p system, which was found to be $C_{{}^7\text{Be}-p,p_{3/2}}^2 = 0.543 \pm 0.027 \text{ fm}^{-1}$. Finally, the astrophysical $S_{17}(0)$ factor was found to be $S_{17}(0) = 20.8 \pm 1.1 \text{ eV b}$.

DOI: [10.1103/PhysRevC.80.064617](https://doi.org/10.1103/PhysRevC.80.064617)

PACS number(s): 25.60.Gc, 25.60.Dz, 21.10.Jx, 25.60.Bx

I. INTRODUCTION

The radiative capture ${}^7\text{Be}(p,\gamma){}^8\text{B}$ reaction plays a major role in the production of high-energy neutrinos in the sun from the β decay of ${}^8\text{B}$. At solar energies (~ 20 keV in the center of mass frame of the ${}^7\text{Be} + p$ system), $E1$ radiative capture is dominant and the $\sigma_{p\gamma}(E_{\text{c.m.}})$ cross section is directly related to the neutrino flux. It is conventional to determine it in terms of the astrophysical factor $S_{17}(E_{\text{c.m.}}) = \sigma_{p\gamma}(E_{\text{c.m.}})E_{\text{c.m.}} \exp(2\pi\eta)$, where η is the Sommerfeld parameter. The overall knowledge about S_{17} for this reaction has improved considerably because of a new direct technique for the proton capture reaction with radiative ${}^7\text{Be}$ targets as well as new radioactive beam facilities for indirect measurements of Coulomb excitation or Coulomb breakup cross sections. The $S_{17}(0)$ value of $21.4 \pm 0.5(\text{exp}) \pm 0.6(\text{theor}) \text{ eV b}$ recommended from the analysis of all the available low-energy data, including recent direct measurements at $E_{\text{c.m.}} = 116\text{--}1244$ keV [1] and $E_{\text{c.m.}} = 302\text{--}1078$ keV [2], and the extrapolation of $\sigma_{p\gamma}(E_{\text{c.m.}})$ to $E_{\text{c.m.}} = 0$, was reported in Ref. [1]. This value is consistent with the extrapolated value of $S_{17}(0) = 21.2 \pm 0.7 \text{ eV b}$ obtained in Ref. [2] from the entire set of measurements. The $S_{17}(0)$ values extracted from the indirectly measured data, which were obtained from the Coulomb breakup, are estimated to be within the range $16.7 \leq S_{17}(0) \leq 20.6 \text{ eV b}$ [3]. Comparing the $S_{17}(0)$ values following from the direct and indirect experiments, one concludes that the results are slightly technique-dependent. Theoretical calculations have to be used to extrapolate the measured S -factor to the astrophysically relevant energies. The recent status of different cluster models used in the field of nuclear astrophysics is presented, for example, in the review of Descouvemont [4].

Indirect measurements related to the Coulomb dissociation of ${}^8\text{B}$ in the field of heavy nuclei proceed predominantly via $E1$ transitions, but a contribution of higher multipoles and the nuclear interaction is also possible because the very first breakup measurement [5], a contribution of $E2$ photons, was intensively studied in a number of experimental and theoretical works [6–8]. A discussion of this problem can be found in Ref. [9].

Important information can be obtained from the study of nuclear reactions with light exotic nuclei, which is related to their structure. It is well known that ${}^8\text{B}$ is an exotic nucleus with a weakly bound proton (0.137 MeV), and the elastic scattering, fusion, and dissociation of ${}^8\text{B}$ in the field of heavy nuclei (in particular, on ${}^{58}\text{Ni}$) are of special interest and were widely studied both experimentally [10–14] and theoretically [15–22].

In this article, we report the results of the ${}^8\text{B} + {}^{58}\text{Ni}$ system analysis with the method of continuum-discretized coupled channels (CDCC) [23–25] in the energy interval 20–28.4 MeV in laboratory system, which are on and slightly above the Coulomb barrier ($V_B = 20.8$ MeV). We carry out the CDCC calculations of the breakup of ${}^8\text{B}$ on ${}^{58}\text{Ni}$ and direct proton transfer for the ${}^8\text{B} + {}^{58}\text{Ni}$ system and compare the results with the differential cross sections measured in Refs. [12,13]. The first aim of our analysis is to study the influence of the ${}^7\text{Be}$ core-target interaction potential on the breakup cross section, for which we employ an optical model fit to the recent data on the elastic scattering angular distributions for the ${}^7\text{Be} + {}^{58}\text{Ni}$ and ${}^8\text{B} + {}^{58}\text{Ni}$ systems measured at five different energies around the Coulomb barrier [14]. Second, applying a reasonable ${}^7\text{Be}$ -target OP and two different ${}^7\text{Be}$ - p relative motion wave functions, we fit the experimental cross section at a ${}^8\text{B}$ laboratory energy of 25.75 MeV [12], with the aim

of extracting an experimental spectroscopic factor (SF) S_{exp} for the ${}^7\text{Be}-p$ system. Then, this value of SF can be used to calculate the excitation function of the ${}^7\text{Be}$ emission in the ${}^8\text{B} + {}^{58}\text{Ni}$ reaction, in comparison with a recent experiment [13], in which the emission of the ${}^7\text{Be}$ products was measured for the forward angle $\theta_{\text{lab}} = 45^\circ$ at 25.0, 26.9, and 28.4 MeV bombarding energies. The result of the analysis is then used to extract the astrophysical $S_{17}(0)$ factor by means of the asymptotic normalization coefficient method.

II. ELASTIC SCATTERING ANALYSIS

Recently, ${}^8\text{B}$ and ${}^7\text{Be} + {}^{58}\text{Ni}$ elastic scattering angular distributions were measured [14] in the angular range $\theta_{\text{c.m.}} = 25^\circ - 158^\circ$ for energies near the Coulomb barrier. The scattering data correspond to ${}^8\text{B}$ laboratory energies of 20.7, 23.4, 25.3, 27.2, and 29.3 MeV and ${}^7\text{Be}$ laboratory energies of 15.1, 17.1, 18.5, 19.9, and 21.4 MeV. The angular distributions for both projectiles show a prominent reduction for $\theta_{\text{c.m.}} > 50^\circ$ because of the flux going to other channels that are associated mainly with breakup. The primary aim of the experiment and its analysis was to compare the elastic and the total reaction cross sections for the proton-halo nucleus ${}^8\text{B}$ and for the “normal,” weakly bound ${}^7\text{Be}$ nucleus using well-adjusted OPs. OPs of Woods-Saxon shape with a shallow real part and a very deep imaginary part for the ${}^8\text{B} + {}^{58}\text{Ni}$ system as well as the Sao Paulo potential [26] for the ${}^7\text{Be} + {}^{58}\text{Ni}$ system were used. The parameters of these OPs were slightly energy-dependent. Lubian *et al.* [22] have also investigated the effects of inelastic excitations of the target and continuum-continuum couplings on the angular distributions by comparison of the experimental ${}^8\text{B} + {}^{58}\text{Ni}$ angular distributions measured in Ref. [14] with results of the respective CDCC model calculations. To describe the ${}^7\text{Be}$ -target interaction, the authors of Ref. [22] adopted the OP of Moroz *et al.* [27], which fit the data of ${}^7\text{Li} + {}^{58}\text{Ni}$ elastic scattering at $E_{\text{lab}} = 20.3$ MeV. It was shown that the simplest calculations involving a single-channel problem, without any type of couplings, are consistent with the data only at the lowest energies of ${}^8\text{B}$ projectiles, $E_{\text{lab}} = 20.7$ and 23.4 MeV. On the other hand, Lubian *et al.* [22] have found that coupling to breakup greatly improves the agreement with experiment, whereas the inelastic excitations of the target do not have an appreciable influence on the elastic angular distributions.

In this article, we carry out a new analysis of the data of Ref. [14] with the aim of finding a single energy-independent set of potential parameters. We apply an OP formalism with the standard complex nuclear OP of the form

$$\mathbf{V}(r) = V_{\text{Coul}}(r) - V_0 \left[1 - F_{\text{s.o.}}(\mathbf{l} \cdot \mathbf{s}) \frac{r_0}{r} \frac{d}{dr} \right] f_0(r) - i \left(W - 4W_D \frac{d}{dr} \right) f_W(r),$$

$$f_i(r) = \{1 + \exp[(r - R_i)/a_i]\}^{-1}, \quad R_i = r_i(A_p^{1/3} + A_T^{1/3}).$$

The Coulomb interaction is represented by the $V_{\text{Coul}}(r)$ potential of a uniformly charged sphere of radius $R_C = r_C(A_p^{1/3} + A_T^{1/3})$.

We performed the coupled-channel calculations using the computer code FRESKO [28]. In our calculations, the coupled-channel equations have been reduced to a single-channel problem, corresponding to the elastic scattering in the entrance channel. We studied a sensitivity of the calculated cross sections to the OP parameters. In particular, we note a strong sensitivity to the parameters that describe a behavior of the potential in the nuclear surface region: the real potential radius and real diffuseness parameter and a very weak sensitivity to the real and imaginary strengths. These features of the OPs explain a possibility of using potentials with the shallow real strengths [14] as well as with deep ones [22]. At the same time, the calculated cross sections depend drastically on the choice of the radial parameter r_0 and can change a few times with r_0 variation of a few (4%–5%) percentage.

Finally, we found the energy-independent OPs producing a good fit to the angular distributions for all energies in this interval for both systems (see Table I). In Figs. 1 and 2, the calculated cross sections for the ${}^7\text{Be} + {}^{58}\text{Ni}$ and ${}^8\text{B} + {}^{58}\text{Ni}$ elastic scattering are compared with the experimental data [14]. These OPs have traditional Woods-Saxon shapes and a depth ratio $V_0/W = 2.5$. The OP describing the ${}^8\text{B} + {}^{58}\text{Ni}$ system has some specific features: a small real diffuseness parameter a_0 and a large imaginary diffuseness parameter a_W . The corresponding long-range imaginary part of the interaction is responsible for the stronger absorption in this system. The optical model and interaction potential parameters compiled in Table I are used in all the calculations carried out in this article.

TABLE I. Optical model and interaction potential parameters.^a

Channel	V_0 (MeV)	$F_{\text{s.o.}}$ (fm)	r_0 (fm)	a_0 (fm)	W (MeV)	W_D (MeV) \times (fm)	r_W (fm)	a_W (fm)	r_C (fm)
${}^8\text{B} + {}^{58}\text{Ni}$	150.0		1.170	0.30	60.0		1.20	0.75	1.20
${}^7\text{Be} + {}^{58}\text{Ni}$	150.0		1.190	0.50	60.0		1.15	0.62	1.20
$p + {}^{58}\text{Ni}$ (OP)	42.6		1.170 ^b	0.75	7.24	2.59	1.26 ^b	0.58	1.25 ^b
$p + {}^{58}\text{Ni}$ (bound)			1.25 ^b	0.75					1.25 ^b
$p + {}^7\text{Be}$ (EB)	44.675	0.351	1.25 ^b	0.52					1.25 ^b
$p + {}^7\text{Be}$ (Kim)	32.120	0.666	1.54 ^b	0.52					1.54 ^b

^a“EB” is the Esbensen and Bertsch potential from Ref. [6]; “Kim” is the Kim *et al.* potential from Ref. [29].

^bThe radii of the potentials are defined as $R_i = r_i A_T^{1/3}$, $i = 0, W, C$.

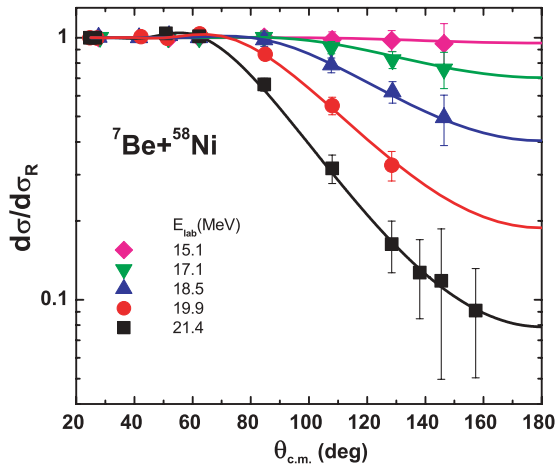


FIG. 1. (Color online) The elastic angular distributions for ${}^7\text{Be} + {}^{58}\text{Ni}$ scattering calculated within the optical model (curves) in comparison with the experimental data [14].

III. ASYMPTOTIC NORMALIZATION COEFFICIENTS AND SPECTROSCOPIC FACTOR RELATION IN CDCC

In a direct reaction, it is convenient to represent the projectile nucleus p as a cluster structure consisting of a core c and a valence fragment v . Thus the main nuclear structure information is contained in the overlap function of cluster configurations $\phi_{cv}(\mathbf{r}) = \langle \psi_c \psi_v | \psi_p \rangle$ [30], which is a model-independent characteristic of the nucleus. This implies that the projectile wave functions $\psi_p(\zeta_p, \mathbf{r})$, where ζ_p denotes all the intrinsic coordinates of the nucleons in the projectile and r is the relative coordinate between a valence fragment v and a core c , may be expanded in terms of the wave functions of the complex subsystems or clusters. A normalization of the overlap functions defines the spectroscopic factor for the vertex $p \rightarrow c + v$:

$$S(p \rightarrow c + v) = \int |\phi_{cv}(\mathbf{r})|^2 dr. \quad (1)$$

The spectroscopic factor S is a measure of the overlaps of the cluster wave functions and gives the probability of the

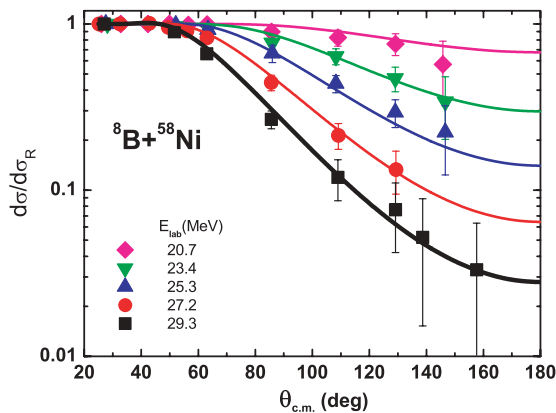


FIG. 2. (Color online) The elastic angular distributions for ${}^8\text{B} + {}^{58}\text{Ni}$ scattering calculated within the optical model (curves) in comparison with the experimental data [14].

wave function $\psi_p(\zeta_p, \mathbf{r})$ of the nucleus p being composed of the wave functions of the clusters c and v with a relative orbital angular momentum l and total angular momentum j . Consequently, the overlap function is not normalized to unity. The asymptotic behavior for $r > R_N$ (R_N is the channel radius) of the radial part $\phi_{cv}(r)$ of the overlap function is determined by the binding energy, ε_{cv} , for the vertex $p \rightarrow c + v$ (see, e.g., Ref. [31]):

$$\phi_{cv}(r) \rightarrow C_{cv,lj} W_{-\eta,l+1/2}(2k_{cv}r)/r \quad (2)$$

$$\phi_{cv}(r) \rightarrow C'_{cv,lj} \sqrt{\frac{2k}{r}} K_{l+1/2}(k_{cv}r), \quad (3)$$

where $k_{cv}^2 = 2\mu_{cv}\varepsilon_{cv}/\hbar^2$ is the relative linear momentum and $\eta = Z_c Z_v e^2 \mu_{cv} / k_{cv}^2$ is the Coulomb parameter. Equation (2), with the Whittaker function, corresponds to the separation of a charged cluster, and Eq. (3), with the modified Bessel function, corresponds to the separation of a neutron. Here $C_{cv,lj}$ and $C'_{cv,lj}$ are the asymptotic normalization coefficients (ANC). For the virtual $p \rightarrow c + v$ vertex, the ANC is related to the nuclear vertex constant (NVC) $G_{cv,lj}$:

$$G_{cv,lj} = -i^l \frac{\sqrt{\pi}}{\mu_{cv}} C_{cv,lj}. \quad (4)$$

The theory and methods for their calculation for light nuclei were developed over 30 years ago and are summarized in the review of Blokhintsev *et al.* [32]. New methods for their evaluation were proposed in Refs. [33–35].

In the CDCC method, the single-nucleon bound state or the state in the continuum of the projectile nucleus p of spin I_p is described by the core + nucleon wave function and is introduced through the parentage expansion,

$$\psi_p(\zeta_c, \mathbf{r}) = \sum_{\alpha} A_{\alpha} [\psi_{I_c}(\zeta_c) \varphi_{\alpha}(\mathbf{r})]_{I_p, M_p}, \quad (5)$$

in terms of the wave functions $\psi_{I_c}(\zeta_c)$ of the core nucleus, of spin I_c , with $(A - 1)$ nucleons. Here A_{α} is the coefficient of fractional parentage and $\varphi_{\alpha}(\mathbf{r})$ is the wave function for the relative $c + v$ motion. The sum includes all states of the core c and valence nucleus v with the angular momentum coupling scheme

$$\mathbf{j} = \mathbf{l} + \mathbf{s} \quad j + I_c = I_p, \quad (6)$$

which we label by $\alpha = \{l, s, j\}$, where l and j denote the relative orbital and total angular momenta of core and valence particle in the projectile and s is the spin of the valence nucleon. In the case of inelastic excitations in the core-valence particle system from the ground state to excited states in the continuum, Eq. (5) describes the bin wave function calculated within a momentum interval, or bin, $[k_{i-1}, k_i]$, labeled by i . The number; the boundaries, k_i ; and the widths $(k_i - k_{i-1})$ of bins are defined by the conditions of an optimal discretization of the continuum for every specific case. The relative wave functions $\varphi_{\alpha}(r)$ for bound and unbound states differ by their asymptotic behavior. The radial bin wave functions $u_{\alpha}(r)$ are square integrable and are calculated as a superposition, within the momentum bin interval $[k_{i-1}, k_i]$, of the eigenfunctions

$f_\alpha(k, r)$ of the $c + v$ internal Hamiltonian; this asymptotic behavior for $r \rightarrow \infty$,

$$f_\alpha(k, r) \rightarrow [\cos \delta_\alpha(k)F_l(kr) + \sin \delta_\alpha(k)G_l(kr)],$$

is described by the regular F_L and irregular G_L Coulomb functions and $k \in [k_{i-1}, k_i]$. To achieve effective normalization of the radial bin wave functions $u_\alpha(r)$, certain weight factors $g_\alpha(k)$ [17] are introduced into the integral over a momentum bin $[k_{i-1}, k_i]$.

The asymptotic behavior of the projectile ground-state bound wave function $u_\alpha(r)$ for $r > R_N$ [cf. Eq. (2)],

$$u_\alpha(r) \rightarrow b_{cv,lj} W_{-\eta,l+1/2}(2kr)/r, \quad (7)$$

is proportional to the “single-particle” ANC $b_{cv,lj}$. The radial parts $u_\alpha(r)$ of the relative $c + v$ motion-bound wave functions $\varphi_\alpha(\mathbf{r})$ are found as the eigenfunctions of a given $V_{cv}(r)$ interaction potential. Commonly, it is generated via a Woods-Saxon potential, the depth of which is adjusted to fit the valence particle separation energy.

In the CDCC method as well as in the distorted wave Born approximation (DWBA), the overlap function $\phi_{cv}(r)$ and the single-particle wave function $u_\alpha(r)$ of the relative motion of c and v fragments describing the bound state of nucleus p are related by

$$\phi_{cv}(r) = S(p \rightarrow c + v)^{1/2} u_\alpha(r) \quad (8)$$

because $u_\alpha(r)$ is normalized to unity. From the comparison of Eqs. (1)–(4), Eq. (7), and Eq. (8), one can deduce, following Ref. [32], that for peripheral direct nuclear reactions, the model-independent NVC and ANC are related to the product of a model-dependent spectroscopic factor (SF) and the “single-particle” ANC $b_{cv,lj}$:

$$G_{cv,lj} = -i^l \frac{\sqrt{\pi}}{\mu_{cv}} C_{cv,lj} \approx -i^l \frac{\sqrt{\pi}}{\mu_{cv}} S_{\text{exp}}(p \rightarrow c + v)^{1/2} b_{cv,lj}. \quad (9)$$

From the first developments of the direct nuclear reaction theory (see, e.g., Refs. [30,32], and references therein), it was noted that the combination $S_{\text{exp}} b^2$, which can be found from DWBA or CDCC analysis of the experimental data, only weakly depends on model parameters, contrary to the behavior of empirical values of SF, S_{exp} , determined by a normalization of the calculated cross section to the experimental data and to the “single-particle” ANC b , separately.

We follow the results that were obtained recently by Capel and Nunes [19]. The authors have shown that the elastic breakup of loosely bound projectile, which is described as a two-body system—a spherical, structureless core c to which a pointlike fragment v is loosely bound—is peripheral in the sense that the breakup cross section is not sensitive to the internal part of the bound wave function for the relative $c + v$ motion. In Ref. [19], breakup calculations were performed for ${}^8\text{B}$ and ${}^{11}\text{Be}$ projectiles at intermediate energies (40–70 MeV/A) on ${}^{208}\text{Pb}$ and ${}^{12}\text{C}$ targets as well as at low energy (26 MeV) on a ${}^{58}\text{Ni}$ target, and it was demonstrated that only the asymptotic properties of the projectile, namely, the ANC of the bound state and the phase shifts in the continuum, influence the breakup cross section.

We emphasize that the ${}^8\text{B}$ breakup and transfer reactions on ${}^{58}\text{Ni}$ at energies around the Coulomb barrier are peripheral in the sense noted previously, with no contribution from the inner part of the ${}^8\text{B}$ bound-state wave function [8,19], because the valence proton is distant from the ${}^7\text{Be}$ by more than the range R_N , where R_N is about 4 fm.

In fact, because $\phi_{cv}(r)$ and $u_\alpha(r)$ may have quite different forms in the inner region, S_{exp} may be quite different from the true spectroscopic factor, $S(p \rightarrow c + v)$, and depend strongly on the choice of $u_\alpha(r)$. Nevertheless, the ANC, $C_{cv,lj} = S_{\text{exp}}(p \rightarrow c + v)^{1/2} b_{cv,lj}$, can be well determined from a peripheral reaction and can serve for the determination of the astrophysical S factor [8]. Thus the cross section from any reaction in which a proton is separated from ${}^8\text{B}$ is proportional to $C_{cv,lj}^2$, as in both the DWBA and the CDCC method.

IV. ${}^8\text{B}$ BREAKUP AND STRIPPING CALCULATIONS AND ASTROPHYSICAL $S_{17}(0)$ FACTOR ESTIMATION

A. ${}^8\text{B}$ breakup

A theoretical analysis within the CDCC model was made for breakup of ${}^8\text{B}$ using the same model space as used in Ref. [17]. We suppose that the proton within ${}^8\text{B}$ has an orbital angular momentum l relative to ${}^7\text{Be}$ and a total angular momentum $\mathbf{j} = \mathbf{l} + \mathbf{s} = \mathbf{l} + 1/2$. Inelastic excitations in the ${}^7\text{Be}$ -proton system from the ground state to excited states with orbital angular momenta $l = 0 - 4$ and energies up to 8 MeV in the continuum were taken into account, and 24, 24, 17, 15, and 15 discretized-continuum states were taken for the $l = 0, 1, 2, 3,$ and 4 states, respectively. The continuum bins were integrated up to $R_{\text{bin}} = 60$ fm, and the CC equations were solved with $R_{\text{max}} = 500$ fm and up to $L_{\text{max}} = 1000$ partial waves using the code FRESKO [28]. The multipoles for the nuclear and Coulomb coupling potentials were included up to $\lambda = 4$. The model space described earlier turns out to give good convergence of the resulting breakup cross sections. The cross sections calculated using FRESKO in the center of mass frame of the projectile and the target were transformed to the laboratory coordinate system related to a measurement of the reaction products with an elastic Jacobian. For the case of the inelastic (breakup) differential cross sections, this transformation gives practically the same result in comparison with the exact method proposed by Tostevin *et al.* [17].

Calculations were performed with the nuclear interaction and OPs shown in Table I. The OP for the p - ${}^{58}\text{Ni}$ scattering was taken from the global parametrization of Becchetti and Greenlees [36]. For the ${}^7\text{Be}$ - ${}^{58}\text{Ni}$ interaction, the OPs obtained from the elastic scattering analysis were used.

The results of the CDCC calculations for the ${}^7\text{Be}$ angular distributions and the experimental data obtained at the University of Notre Dame [12] at $E_{\text{lab}} = 25.75$ MeV are shown in Fig. 3. This figure also shows a comparison of the CDCC calculations made using two sets of optical parameters for the core-target interaction: the ${}^7\text{Be} + {}^{58}\text{Ni}$ and ${}^8\text{B} + {}^{58}\text{Ni}$ OPs from Table I. Two values of spectroscopic factors ($S_{\text{exp}} = 1$ and $S_{\text{exp}} = 1.1025$) and the EB bound-state wave function were used. One can see that the calculated breakup differential cross

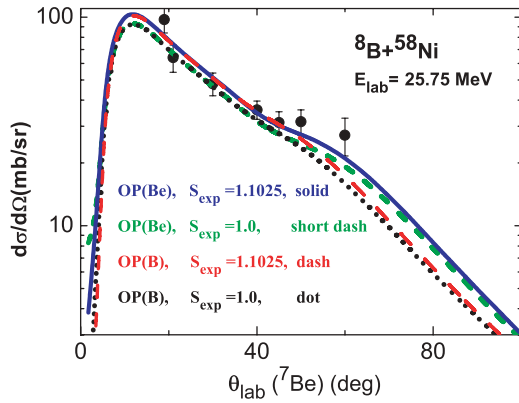


FIG. 3. (Color online) The CDCC calculations for the ${}^7\text{Be}$ differential cross sections from the ${}^8\text{B} + {}^{58}\text{Ni}$ breakup reaction at $E_{\text{lab}} = 25.75$ MeV, using the ${}^7\text{Be} + {}^{58}\text{Ni}$ and ${}^8\text{B} + {}^{58}\text{Ni}$ OPs from Table I and for two values of spectroscopic factors: $S_{\text{exp}} = 1$ and $S_{\text{exp}} = 1.1025$, in comparison with the experimental data [12].

sections are less sensitive to the choice of the core-target OP at the maximum of the angular distribution, as it has been noted in Ref. [17], but the main difference between the calculations carried out with these different OPs is seen for the middle angles $40^\circ < \theta_{\text{lab}} < 100^\circ$.

The spectroscopic factor $S_{\text{exp}}({}^8\text{B} \rightarrow {}^7\text{Be} + p)$ was estimated by a comparison of the experimental and calculated differential cross sections. As mentioned earlier, the normalization of the calculated cross section depends on the choice of the $p + {}^7\text{Be}$ bound-state wave function. The variation of the geometric parameters of the $p + {}^7\text{Be}$ interaction potential can significantly change the normalization of the cross section and thus the spectroscopic factor. In particular, an increase of the $p + {}^7\text{Be}$ interaction radius leads to a decrease in the $S_{\text{exp}}({}^8\text{B} \rightarrow {}^7\text{Be} + p)$ value. The “single-particle” asymptotic normalization coefficient b is obviously model-dependent because it is well characterized by the geometry of the potential. Nevertheless, as shown in Refs. [37,38], if one varies both geometric parameters, the radius and diffuseness, of the single-particle potential, leaving the single-particle ANC b constant, the breakup cross section does not change. In Ref. [38], this method was applied to determine the correct ANC in the ${}^7\text{Be}(p, \gamma){}^8\text{B}$ reaction and to estimate the astrophysical S_{17} factor.

In our analysis, two normalized single-particle ${}^7\text{Be} + p$ wave functions generated by two Woods-Saxon potentials (see Table I) and adjusted to fit the proton separation energy of $E_B = 0.137$ MeV were used. The first was tested in Ref. [6] for the radiative capture calculations of the ${}^7\text{Be}(p, \gamma){}^8\text{B}$ reaction cross sections and the second was applied in Ref. [29]. These wave functions are very different because the Kim interaction potential has a larger radius. We assume that the 2^+ ground state (g.s.) of ${}^8\text{B}$ is described by a $p_{3/2}$ proton wave function coupled to the $3/2^-$ g.s. of the ${}^7\text{Be}$ core. The ${}^8\text{B}(\text{g.s.})$ wave function generated by the EB potential has a single-particle ANC $b = 0.7005 \text{ fm}^{-1/2}$, and the ${}^8\text{B}(\text{g.s.})$ wave function generated by the Kim potential has a single-particle ANC $b = 0.8013 \text{ fm}^{-1/2}$.

We obtained the best fits to the experimental data at $E_{\text{lab}} = 25.75$ MeV [12] by the CDCC breakup calculations with a spectroscopic factor for the ${}^8\text{B} \rightarrow {}^7\text{Be} + p$ vertex $S_{\text{exp}}({}^8\text{B} \rightarrow {}^7\text{Be} + p) = 1.1025$ using the EB wave function and $S_{\text{exp}}({}^8\text{B} \rightarrow {}^7\text{Be} + p) = 0.85$ using the Kim wave function. The calculated curves are practically indistinguishable (see Fig. 3).

The main result is that the ANC $C_{\text{Be-}p, p_{3/2}}$ was found to be essentially the same for both wave functions used in the calculations: $C_{\text{Be-}p, p_{3/2}}^2 = 0.541 \text{ fm}^{-1}$ for the EB wave function and $C_{\text{Be-}p, p_{3/2}}^2 = 0.545 \text{ fm}^{-1}$ for the Kim wave function. The uncertainty of the spectroscopic factor estimation is within 5%, and the average value of the ANC that we accept for the following calculations is $C_{\text{Be-}p, p_{3/2}}^2 = 0.543 \pm 0.027 \text{ fm}^{-1}$; $C_{\text{Be-}p, p_{3/2}} = 0.737 \pm 0.018 \text{ fm}^{-1/2}$. This value is in perfect accord with the theoretical analysis of the latest direct S -factor determination given in Ref. [38]: $(C_{p_{3/2}}^{\text{exp}})^2 = 0.558 \pm 0.015 \text{ fm}^{-1}$. It also coincides with the $C_{\text{Be-}p, p_{3/2}} = 0.740 \text{ fm}^{-1/2}$ obtained in Ref. [8] from a CDCC analysis of the ${}^8\text{B}$ breakup on ${}^{208}\text{Pb}$ at 52 MeV/nucleon.

B. Proton transfer

In the recent article of Aguilera *et al.* [14], the ${}^8\text{B} + {}^{58}\text{Ni}$ reaction cross section was studied, and interesting results about the proton halo properties of ${}^8\text{B}$ were obtained. The total reaction cross section found for the ${}^8\text{B} + {}^{58}\text{Ni}$ system shows a very large enhancement with respect to the predictions typically expected for weakly bound “normal” nuclei, for instance, Li and Be projectiles. This behavior of the ${}^8\text{B} + {}^{58}\text{Ni}$ cross section is very similar to the cross section enhancement observed for the interaction of the neutron halo nucleus ${}^6\text{He}$ (${}^6\text{He} + {}^{209}\text{Bi}$, ${}^6\text{He} + {}^{64}\text{Zn}$). In contrast to the ${}^6\text{He}$ -induced reactions, where most of the reaction yield comes from two-neutron transfer to neutron-unbound levels, the enhancement in the ${}^8\text{B}$ -induced total reaction cross section comes mainly through the long-range Coulomb plus nuclear breakup force, and proton transfer is not expected for a proton halo system. Nevertheless, we would like to estimate the contribution from the direct proton transfer to the bound states of ${}^{59}\text{Cu}$ because this process can contribute to the total ${}^7\text{Be}$ yield.

In accordance with the aim of this work, to obtain a complete description of the experimental data and spectroscopic information, we performed calculations of the differential cross sections of the direct proton transfer to the bound states in ${}^{59}\text{Cu}$ in the exact finite-range DWBA using the FRESKO computer code. The shell-model studies of Cu isotopes [39] showed that ${}^{59}\text{Cu}$ can be rather well described by an inert core with one extra proton particle and two valence neutrons outside the core. The ground state of ${}^{59}\text{Cu}$ is $3/2^-$, and it conforms to the occupation of the $2p_{3/2}$ oscillator orbital. The low-lying states in near-semimagic nuclei usually carry a major part of the proton single-particle strength. We consider the direct proton transfer to some states of ${}^{59}\text{Cu}$ with spin and parity quantum numbers of the valence proton above the $Z = 28$ shell: $2p_{3/2}$, $1f_{5/2}$, $2p_{1/2}$, $1g_{9/2}$, and some other states for which the experimental spectroscopic strength, following from the analysis of (d, n) reactions [40], are most important. We use

TABLE II. Total j_2 , orbital l_2 angular momenta, and a number of nodes N_2 of the bound-state wave functions for the $^{59}\text{Cu} \rightarrow ^{58}\text{Ni} + p$ vertex, and the proton spectroscopic factors of the lowest states in ^{59}Cu .

$E_x(\text{MeV})$	$I_{^{59}\text{Cu}}^\pi$	j_2	l_2	N_2	\tilde{S}^a
0.0	$3/2^-$	$3/2$	1	2	1.85
0.491	$1/2^-$	$1/2$	1	2	0.84
0.914	$5/2^-$	$5/2$	3	1	2.5
1.398	$7/2^-$	$7/2$	3	1	0.4
2.319	$1/2^-$	$1/2$	1	2	0.1
3.043	$9/2^+$	$9/2$	4	1	2.4

^a $\tilde{S} = (2I_f + 1)C^2S$; here C^2 is the isospin Clebsch-Gordan coefficient.

the same OPs (Table I) as for the scattering calculations. The normalized single-particle $^7\text{Be} + p$ wave function generated by a EB Woods-Saxon potential (Table I) is used to describe the bound-state relative motion of $^7\text{Be} + p$ in ^8B .

We take into account the standard angular-momentum coupling scheme (see, e.g., Ref. [30])

$$\begin{aligned} \mathbf{I}_a &= \mathbf{I}_b + \mathbf{j}_1, & \mathbf{I}_f &= \mathbf{I}_A + \mathbf{j}_2, \\ \mathbf{j}_1 &= \mathbf{s}_p + \mathbf{l}_1, & \mathbf{j}_2 &= \mathbf{s}_p + \mathbf{l}_2 \\ \mathbf{L} &= \mathbf{j}_1 + \mathbf{j}_2 = \mathbf{l}_1 + \mathbf{l}_2, \end{aligned} \quad (10)$$

to describe the direct stripping mechanism $^8\text{B}(I_a) + ^{58}\text{Ni}(I_A) \rightarrow [^7\text{Be} + p(s_p)] + ^{58}\text{Ni} \rightarrow ^7\text{Be} + [p(s_p) + ^{58}\text{Ni}] \rightarrow ^7\text{Be}(I_b) + ^{59}\text{Cu}(I_f)$ of the reaction $^{58}\text{Ni}(^8\text{B}, ^7\text{Be})^{59}\text{Cu}$. Here \mathbf{L} is the transferred angular momentum; \mathbf{l}_1 and \mathbf{l}_2 are orbital angular momenta of relative motion of the proton in the nuclei ^8B and ^{59}Cu , respectively; and \mathbf{j}_1 and \mathbf{j}_2 are total transferred angular momenta.

For the case of the $^{58}\text{Ni}(^8\text{B}, ^7\text{Be})^{59}\text{Cu}$ reaction, the angular momentum and parity values are $I_A^\pi = 0^+$, $I_a^\pi = 2^+$, $I_b^\pi = 3/2^-$, $j_1 = 3/2$, and $l_1 = 1$. The experimental proton spectroscopic factors for these states [39,40], which were used in our calculations, are shown in Table II.

Figure 4 shows the contribution of the direct proton transfer mechanism (dotted line) to the cross section for ^7Be production in the $^{58}\text{Ni}(^8\text{B}, ^7\text{Be})$ reaction at $E_{\text{lab}} = 25.75$ MeV. The solid line represents the incoherent sum of the breakup and stripping mechanisms.

This calculation shows that proton stripping provides approximately 5% of the total ^7Be emission cross sections. This result confirms the intuitive expectation declared in Ref. [14]. Nevertheless, the maximum contribution to the cross section falls in the angular interval from 50° to 80° and provides a slightly improved description of the local maximum in the experimental differential cross section at $\theta_{\text{lab}} \approx 50^\circ$.

C. Excitation function

The integrated breakup cross section obtained in Ref. [14] from the CDCC calculation for the $^8\text{B} + ^{58}\text{Ni}$ system reproduces the measured breakup yield at $E_{\text{lab}} = 25.8$ MeV quite well. There is a slightly enhanced energy dependence in the energy interval from $E_{\text{lab}} \approx 20$ – 29 MeV. In this article,

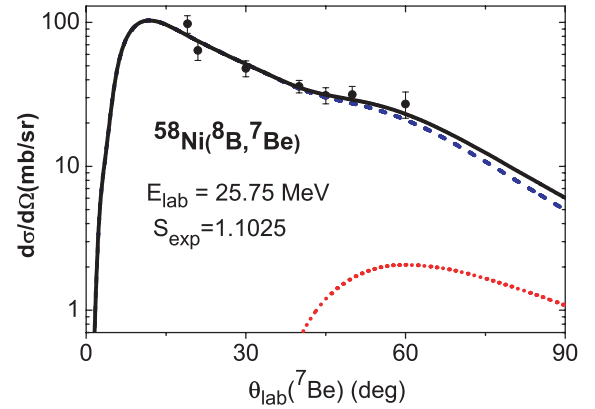


FIG. 4. (Color online) The contribution of the direct proton transfer mechanism (dotted line) comparing with the breakup cross section (dashed line). The incoherent sum of both cross sections and the experimental data of Kolata *et al.* [12] are shown by the solid line and the data points, respectively.

we present a detailed analysis of the energy dependence of the differential cross sections for this system. Figure 5 shows the results of CDCC calculations at $E_{\text{lab}} = 20.7, 23.4, 25.0, 25.75, 26.9,$ and 28.4 MeV. For comparison purposes, the experimental differential cross sections for the $^{58}\text{Ni}(^8\text{B}, ^7\text{Be})$ reaction reported in Ref. [12] at a beam energy of 25.75 MeV are also shown. The theoretical curves represent the incoherent sum of the breakup and proton-transfer mechanisms. It is observed that the calculations predict a sufficient increase with energy of the cross sections for breakup at their maxima near $\theta_{\text{lab}} \approx 12^\circ$. A relative increase of the cross section near $\theta_{\text{lab}} \approx 45^\circ$ is also seen in Fig. 5, especially at $E_{\text{lab}} = 28.4$ MeV.

The energy dependence of the cross section of the ^7Be product emission at $\theta_{\text{lab}} = \pm 45^\circ$ was measured in a recent experiment, performed using the TwinSol facility at the University of Notre Dame [13]. ^8B beams with $E_{\text{lab}} = 25.0, 26.9,$ and 28.4 MeV were scattered on a ^{58}Ni target. The 45° excitation function calculated at six energies, mentioned earlier for the breakup and proton-transfer channels, are shown in the lower part of Fig. 6, in comparison with the data for the $^8\text{B} + ^{58}\text{Ni}$ reaction. The calculations performed without any energy dependence of the potential parameters demonstrate a growth of the cross section with energy, which can also be seen in the experimental data. The $\sim 12^\circ$ (maximum of the angular distribution) excitation function and integrated cross sections are also shown in Fig. 6. It is observed that the magnitude of the cross section at the maximum of the angular distribution increases more rapidly with energy than the second maximum near 45° and the integrated cross section as a whole. The integrated cross section (the upper curve in Fig. 6) is practically the same as the one indicated by the dotted line (CDCC calculations) in Ref. [14].

D. $S_{17}(0)$ factor estimation

Let us now apply the results obtained from the ^8B breakup and stripping calculations to estimate the astrophysical $S_{17}(0)$ factor based on the potential model developed in Refs. [41,42].

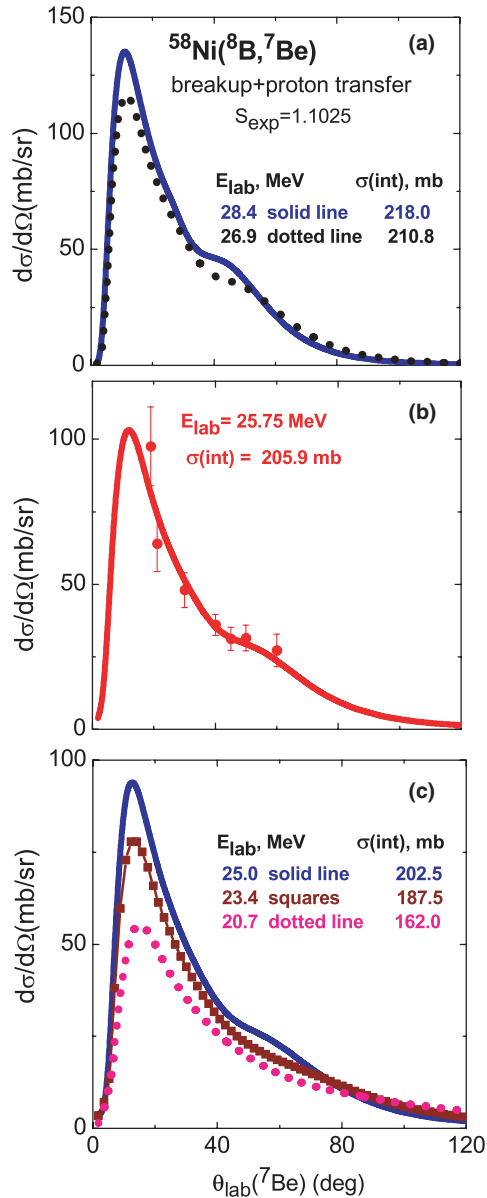


FIG. 5. (Color online) Breakup plus direct proton transfer cross sections calculated at (a) $E_{\text{lab}}(^8\text{B}) = 28.4$ and 26.9 MeV, (b) $E_{\text{lab}}(^8\text{B}) = 25.75$ MeV, and (c) $E_{\text{lab}}(^8\text{B}) = 25.0$, 23.4 , and 20.7 MeV. The data points are from Ref. [12].

At very low incident energies, the proton capture reaction ${}^7\text{Be}(p, \gamma){}^8\text{B}$ leading to the ground state of ${}^8\text{B}$ is extremely peripheral because of the Coulomb barrier. The amplitude of the reaction, therefore, depends on the overlap between the ground-state wave functions of ${}^7\text{Be}$ and ${}^8\text{B}$ only in the tail region, where the radial part of the overlap has the form of Eq. (2). The cross sections $\sigma_{p\gamma}(0)$, and consequently, $S_{17}(0)$, are proportional to $C_{\text{Be-}p}^2$. An accurate approximation of the $S_{17}(E)$ at very low energies was obtained in Refs. [41,42], taking into account the asymptotic behavior of the $p + {}^7\text{Be}$ scattering wave function and its derivatives at zero energy. The model-independent analytical expression for $S_{17}/C_{\text{Be-}p}^2$ (assuming that the initial scattering wave function at zero energy can be replaced by its asymptotic form) corresponding

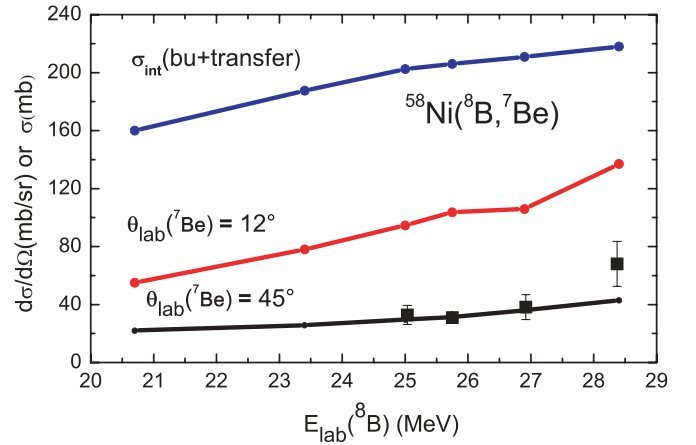


FIG. 6. (Color online) Energy dependence of the breakup plus direct proton transfer cross sections calculated at the six energies. The upper line shows the integrated cross sections; the middle line corresponds to the maxima of the differential cross sections; the lower line and points illustrate a comparison between calculated and measured in Ref. [13] differential cross sections at an angle of 45° , respectively.

to the external capture process takes the form

$$S_{17}(0)/C_{\text{Be-}p}^2 \approx 38.0(1 - 0.0013a_0) \text{ eV b fm}, \quad (11)$$

where s and d waves of the relative ${}^7\text{Be} + p$ motion were incorporated into the overlap integral.

The main unknown parameter of the model is the scattering length a_0 , which was taken to be the average value of the scattering lengths a_{01} and a_{02} for the channel spins $I = 1$ and $I = 2$. In recent calculations [8,38], this average value varies between -2 and -7 fm. The theoretical error of $S_{17}(0)$ associated with this range of a_0 does not exceed 0.3% and is therefore negligible compared with the errors following from the uncertainties in the determination of other parameters. In our calculation, we take $a_0 = -7$ fm, following Ref. [38].

Finally, according to Eq. (9) and taking into account the estimated errors of 5.3% , we find that $S_{17}(0) = 20.8 \pm 1.1$ eV b. This value is in perfect accord with the value of $S_{17}(0) = 20.9 \pm 2.0(\text{exp}) \pm 1.9(\text{theor})$ eV b obtained in Ref. [8]. Comparing with the $S_{17}(0)$ approximations of the direct and indirect data, we conclude that our estimation is a bit smaller than those obtained from the direct data [1] (though it lies inside the error bar) and corresponds to the upper limit of the $S_{17}(0)$ values obtained from the indirect data [3].

V. CONCLUSIONS

The process of ${}^8\text{B}$ breakup in the field of heavy nuclei is of special interest as it can provide the cross section for the ${}^7\text{Be}$ radiative proton capture at low energies, a reaction that is essential for the understanding of a solar neutrino emission. The astrophysical $S_{17}(0)$ factor extracted from the indirectly measured Coulomb breakup data is estimated to be within the range $16.7 \leq S_{17}(0) \leq 20.6$ eV b, whereas recent values obtained from the direct measurements are in the range 21.2 – 21.4 eV b.

We have performed CDCC calculations for the breakup of ${}^8\text{B}$ on ${}^{58}\text{Ni}$, and direct proton transfer for the ${}^8\text{B} + {}^{58}\text{Ni}$ system, at energies of 20–28.4 MeV, which are on and slightly above the Coulomb barrier. The influence of the ${}^7\text{Be}$ core-target OP on the breakup cross section was investigated. For this purpose, the recent data on the elastic scattering angular distributions for the ${}^7\text{Be}$ - ${}^{58}\text{Ni}$ and ${}^8\text{B}$ - ${}^{58}\text{Ni}$ systems measured at five different energies around the Coulomb barrier were analyzed. The data were fit within the optical model, and a reasonably energy-independent OP for each system, which allows a good fit to the experimental angular distributions in this energy interval, was obtained. After applying these OPs and two different ${}^7\text{Be} + p$ relative motion wave functions, and summing breakup and direct proton transfer contributions, we were able to fit the experimental cross section at a ${}^8\text{B}$ laboratory energy of 25.75 MeV [12] and to extract the spectroscopic factors S_{exp} for the ${}^7\text{Be}$ - p system corresponding to the two specific choices for the ${}^7\text{Be} + p$ bound-state wave functions. The S_{exp} value was used to calculate the excitation function of the breakup of ${}^8\text{B}$ on ${}^{58}\text{Ni}$, in comparison with the recent experiment [13], in which ${}^7\text{Be}$ products were measured at the forward angle of $\theta_{\text{lab}} = 45^\circ$ for $E_{\text{lab}} = 25.0, 26.9,$ and 28.4 MeV.

In view of the peripheral character of the ${}^8\text{B}$ breakup reaction at near-barrier energies, the asymptotic normalization coefficient $C_{\text{Be-}p,p_{3/2}}$ was calculated by the relation $C^2 = S_{\text{exp}} b^2$, where b is a single-particle ANC following from the adopted ${}^7\text{Be} + p$ single-particle wave functions. The ANC was found to be $C_{\text{Be-}p,p_{3/2}}^2 = 0.543 \pm 0.027 \text{ fm}^{-1}$, independently of the choice of the ${}^7\text{Be} + p$ bound-state wave function. Finally, the astrophysical $S_{17}(0)$ factor was found to be $S_{17}(0) = 20.8 \pm 1.1 \text{ eV b}$. This value lies between the experimental values obtained from the direct and indirect data and is in accordance with the value obtained from the similar CDCC analysis of the ${}^8\text{B}$ breakup on ${}^{208}\text{Pb}$ data at 52 MeV/A [8].

ACKNOWLEDGMENTS

This work was partially supported by project 2428/2007 (UAEMex, Mexico), by CONACyT (Mexico), and by the US NSF under Grant No. PHY06-52591. A.M.M. is supported by the Spanish Ministerio de Ciencia e Innovación under project FPA2006-13807-c02-01 and by the Spanish Consolider-Ingenio 2010 Programme CPAN (Grant No. CSD2007-00042).

-
- [1] A. R. Junghans, M. C. Mohrmann, K. A. Snover *et al.*, Phys. Rev. Lett. **88**, 041101 (2002); A. R. Junghans, M. C. Mohrmann, K. A. Snover *et al.*, Phys. Rev. C **68**, 065803 (2003).
- [2] L. T. Baby, C. Bordeanu, G. Goldring *et al.*, Phys. Rev. Lett. **90**, 022501 (2003); Phys. Rev. C **67**, 065805 (2003).
- [3] F. Schumann *et al.*, Phys. Rev. C **73**, 015806 (2006).
- [4] P. Descouvemont, J. Phys. G **35**, 014006 (2008).
- [5] T. Motobayashi *et al.*, Phys. Rev. Lett. **73**, 2680 (1994).
- [6] H. Esbensen and G. Bertsch, Nucl. Phys. **A600**, 37 (1996).
- [7] H. Esbensen, G. F. Bertsch, and K. A. Snover, Phys. Rev. Lett. **94**, 042502 (2005).
- [8] K. Ogata, S. Hashimoto, Y. Iseri, M. Kamimura, and M. Yahiro, Phys. Rev. C **73**, 024605 (2006).
- [9] B. Davids and S. Typel, Phys. Rev. C **68**, 045802 (2003).
- [10] J. von Schwarzenberg, J. J. Kolata, D. Peterson, P. Santi, M. Belbot, and J. D. Hinnefeld, Phys. Rev. C **53**, R2598 (1996).
- [11] V. Guimarães *et al.*, Phys. Rev. Lett. **84**, 1862 (2000).
- [12] J. J. Kolata *et al.*, Phys. Rev. C **63**, 024616 (2001).
- [13] E. F. Aguilera, E. Martinez-Quiroz, T. L. Belyaeva, J. J. Kolata, and R. Leyte-Gonzalez, Phys. At. Nucl. **71**, 1191 (2008).
- [14] E. F. Aguilera *et al.*, Phys. Rev. C **79**, 021601(R) (2009).
- [15] F. M. Nunes and I. J. Thompson, Phys. Rev. C **57**, R2818 (1998); **59**, 2652 (1999).
- [16] H. Esbensen and G. F. Bertsch, Phys. Rev. C **59**, 3240 (1999).
- [17] J. A. Tostevin, F. M. Nunes, and I. J. Thompson, Phys. Rev. C **63**, 024617 (2001).
- [18] A. M. Moro and F. M. Nunes, Nucl. Phys. **A767**, 138 (2006).
- [19] P. Capel and F. M. Nunes, Phys. Rev. C **75**, 054609 (2007).
- [20] D. Baye, Eur. Phys. J. Spec. Top. **156**, 93 (2008).
- [21] J. Lubian, T. Correa, P. R. S. Gomes, and L. F. Canto, Phys. Rev. C **78**, 064615 (2008).
- [22] J. Lubian, T. Correa, E. F. Aguilera, L. F. Canto, A. Gomez-Camacho, E. M. Quiroz, and P. R. S. Gomes, Phys. Rev. C **79**, 064605 (2009).
- [23] M. Kamimura *et al.*, Prog. Theor. Phys. Suppl. **89**, 1 (1986).
- [24] N. Austern *et al.*, Phys. Rep. **154**, 125 (1987).
- [25] I. J. Thompson, Comput. Phys. Rep. **7**, 167 (1988).
- [26] L. C. Chamon *et al.*, Phys. Rev. C **66**, 014610 (2002).
- [27] Z. Moroz *et al.*, Nucl. Phys. **A381**, 294 (1982).
- [28] I. J. Thompson, FRESCO user's manual and code (available from author).
- [29] K. H. Kim, M. H. Park, and B. T. Kim, Phys. Rev. C **35**, 363 (1987).
- [30] G. R. Satchler, *Direct Nuclear Reactions* (Clarendon Press, Oxford, 1983).
- [31] C. Bertulani, Rev. Mex. Fis. **S54**, 11 (2008); J. Huang, C. A. Bertulani, and V. Guimaraes, At. Data Nucl. Data Tables (to be published).
- [32] L. D. Blokhintsev, I. Borbely, and E. I. Dolinskii, Fiz. Elem. Chastits At. Yadra **8**, 1189 (1977) [Sov. J. Part. Nucl. **8**, 485 (1977)].
- [33] L. D. Blokhintsev and V. O. Yeremenko, Phys. At. Nucl. **71**, 1219 (2008).
- [34] H. M. Xu, C. A. Gagliardi, R. E. Tribble, A. M. Mukhamedzhanov, and N. K. Timofeyuk, Phys. Rev. Lett. **73**, 2027 (1994).
- [35] A. M. Mukhamedzhanov and F. M. Nunes, Phys. Rev. C **72**, 017602 (2005); D. Y. Pang, F. M. Nunes, and A. M. Mukhamedzhanov, *ibid.* **75**, 024601 (2007).
- [36] F. D. Becchetti and G. W. Greenlees, Phys. Rev. **182**, 1190 (1969).
- [37] S. B. Igamov and R. Yarmukhamedov, Nucl. Phys. **A781**, 247 (2007).
- [38] S. B. Igamov and R. Yarmukhamedov, Phys. At. Nucl. **71**, 1740 (2008).
- [39] N. A. Smirnova, A. De Maesschalck, A. Van Dyck, and K. Heyde, Phys. Rev. C **69**, 044306 (2004).
- [40] J. Bommer *et al.*, Nucl. Phys. **A199**, 115 (1973).
- [41] D. Baye and E. Brainis, Phys. Rev. C **61**, 025801 (2000).
- [42] D. Baye, Phys. Rev. C **62**, 065803 (2000).